Sign-changed-magnetostriction effect of morphotropic phase boundary in pseudobinary DyCo_{2}-DyFe_{2} Laves compounds

Tianyu Ma, Xiaolian Liu, Junming Gou, Yue Wang, Chen Wu, Chao Zhou, Yu Wang, Sen Yang, and Xiaobing Ren

Phys. Rev. Materials **3**, 034411 — Published 29 March 2019

DOI: 10.1103/PhysRevMaterials.3.034411

Sign-changed-magnetostriction effect of morphotropic phase boundary in pseudobinary $DyCo_2$-$DyFe_2$ Laves compounds

Tianyu Ma,[1, *] Xiaolian Liu,[1, 4] Junming Gou,[1] Yue Wang,[2] Chen Wu,[2] Chao Zhou,[3] Yu Wang,[3] Sen Yang [3,*] and Xiaobing Ren [1]

[1] *Frontier Institute of Science and Technology and State Key Laboratory for Mechanical Behavior of Materials, Xi'an Jiaotong University, Xi'an 710049, China*

[2] *School of Materials Science and Engineering, Zhejiang University, Hangzhou 310027, China*

[3] *MOE Key Laboratory for Nonequilibrium Synthesis and Modulation of Condensed Matter, School of Science, Xi'an Jiaotong University, Xi'an 710049, China*

[4] *Innovative Center for Advanced Materials, Hangzhou Dianzi University, Hangzhou 310012, China*

[*] Corresponding author. E-mail addresses: matianyu@xjtu.edu.cn (Prof. T. Ma) and yang.sen@xjtu.edu.cn (Prof. S. Yang).

Abstract

Morphotropic phase boundary (MPB) has recently attracted considerable interest in a number of pseudobinary RT_2 (R is rare earth; T is 3d-transition metal) Laves phase compounds to achieving enhanced large magnetostriction or near zero magnetostriction. Unlike the MPBs separating a tetragonal and a rhombohedral phase in the literatures, here we report that in the $DyCo_2$-$DyFe_2$ system, ferromagnetic MPB separating two tetragonal phases of differed tetragonality can also lead to sign-changed-magnetostriction effect. Synchrotron x-ray diffraction data demonstrate the coexistence of two tetragonal phases in the broadening MPB regime, one with $c/a < 1$ (T1 phase) and the other with $c/a > 1$ (T2 phase). The preferable domain switches of T1 phase with weaker magnetocrystalline anisotropy under low fields and the subsequent domain switches of T2 phase with stronger magnetocrystalline anisotropy under high fields give rise to the sign-changed-magnetostriction effect. Further analysis suggests that the MPB effect on magnetostrictive response is determined by the intrinsic magnetostriction, the magnetocrystalline anisotropy as well as the magnetic ordering of two end terminals that form the MPB. This work reveals a new type MPB in pseudobinary RT_2 compounds and provides an effective recipe for designing sign-tunable magnetostrictive materials.

Keywords: Magnetic Materials; Rare-earth Laves phase compounds; Magnetostriction; Magnetic transition

I. INTRODUCTION

The RT_2 rare-earth transition-metal Laves phase compounds have attracted intensive interest in both condensed-matter physics and functional materials due to their diverse physical phenomena including magnetoelastic, magnetocaloric and magnetoelectric effects [1-11]. Since the early 1970s, the pseudobinary $RR'T_2$ (R and R' refer to two rare earth elements) compounds have been the icon of a large class of technologically important materials — magnetostrictive materials, which can convert between magnetic field (magnetization) and mechanical stress (strain) [1-5, 12-19]. The most famous one is the $TbFe_2$-$DyFe_2$ system (typical composition $Tb_{0.3}Dy_{0.7}Fe_2$, known as Terfenol-D) [2, 13], for which the compensation of magnetocrystalline anisotropy at certain composition /temperature conditions can facilitate giant and slim-hysteretic magnetostriction λ_s of ~ 2000 ppm under modest magnetic fields. It has been widely used in fast speed valves, highly sensitive sensors and adaptive vibration control actuators, etc. [20-22].

Recent synchrotron x-ray diffraction (S-XRD) investigations on the pseudobinary $TbFe_2$-$DyFe_2$ and $TbCo_2$-$DyCo_2$ systems with spontaneous magnetization M_s // <111> for one terminal and M_s // <001> for the other [23-25] have suggested that the maximum magnetostriction is associated with a structural transition from rhombohedral phase to tetragonal phase (on cooling). A ferromagnetic morphotropic phase boundary (MPB) is formed in the temperature-composition phase diagram, analogous to the long-established MPB of the physically parallel ferroelectrics that separates two ferroelectric phases with rhombohedral and tetragonal structures [26-29]. More recently, ferromagnetic MPB has also been found in other pseudobinary RT_2 systems, such as $TbCo_2$-$GdCo_2$ [30], $TbFe_2$-$GdFe_2$ [31], and $TbCo_2$-$NdCo_2$ [32]. The ferromagnetic MPB inherits the notable characteristics of MPB in ferroelectrics and share common features including the nearly isotropic total free energy landscape and the coexistence of two highly strained phases. The small free energy barrier

between the two coexisting phases results in nano-sized domains, thus facilitating easy magnetization rotation under low external fields [33, 34]. Consequently, the pseudobinary RT_2 compounds at MPB usually exhibit high magnetic susceptibility and small coercivity field. Unlike the ferroelectric MPB that usually enhances the field-induced strain, however, the available ferromagnetic MPBs can either enhance or weaken the magnetostriction, depending on the magnetic ordering of two end terminals that form the ferromagnetic MPBs. Enhanced magnetostriction effect has been found in the $TbFe_2$-$DyFe_2$ and $TbCo_2$-$DyCo_2$, whereas the MPB in the $TbCo_2$-$GdCo_2$ weakens the magnetostriction. Under external fields, it has been suggested that the state at MPB tends to shift towards the terminal with higher magnetic ordering degree [30]. For the $TbFe_2$-$DyFe_2$ and $TbCo_2$-$DyCo_2$, the state at MPB tends to shift to the rhombohedral side with a larger lattice distortion than the tetragonal terminal, so that the magnetostriction will be enhanced. While for the $TbCo_2$-$GdCo_2$, the tetragonal side exhibits higher magnetic ordering degree but smaller lattice distortion than the rhombohedral side, the shift of MPB leads to near zero magnetostriction [30]. The zero magnetostriction pseudobinary compounds may serve as soft magnets. These advances suggest that adjusting the two end RT_2 terminals of differing structure/magnetic ordering at MPB enables one to tune the magnetostrictive properties for different engineering applications.

Here we report a new ferromagnetic MPB in the pseudobinary $DyCo_2$-$DyFe_2$ system that yields sign-changed-magnetostriction effect, i.e. the magnetostriction sign changes with the increment of magnetic field strength, as shown in Fig.1. The two end terminals $DyFe_2$ and $DyCo_2$ possess the same tetragonal symmetry (with M_S // [001]) but different tetragonalities and magnetic ordering degrees ($c/a < 1$ and $T_C = 140$ K for $DyCo_2$ [35], $c/a > 1$ and $T_C = 635$ K for $DyFe_2$ [36]). The unique sign-changed-magnetostriction ("W" shape λ-H curve) is observed within a broadening MPB region. Such effect stems from the preferable variant reorientations of T1 phase with weaker magnetocrystalline anisotropy and the subsequent

variant reorientations of T2 phase with stronger magnetocrystalline anisotropy, which is potential to facilitate novel applications.

II. EXPERIMENTAL METHODS

A series of (1-x)$DyCo_2$-x$DyFe_2$ (x = 0, 0.08, 0.16, 0.24, and 1) compounds have been designed. The ingots were prepared by arc melting Dy (99.99%), Co (99.95%) and Fe (99.95%) metals under the protection of high-purity argon. To ensure homogeneity, the ingots were melted for six times and subjected to further annealing for 3 days at 1273 K in vacuum-sealed quartz tubes. The annealed samples are polycrystalline, with the mean grain size of ~100 μm. Temperature dependent magnetization (*M* - *T*) curves above room temperature were measured using a Lakeshore 7407 Vibrating Sample Magnetometer (VSM). AC susceptibility versus temperature curves were measured using a Quantum Design 10-6S-9T physical property measurement system (PPMS) magnetometer over the temperature range from 10 to 350 K. Isothermal magnetization hysteresis loops were also measured using the PPMS magnetometer upon *in situ* cooling to certain temperatures. *In situ* temperature-dependent magnetostrictions were measured using the standard strain-gauge technique by zero-field cooling the sample to different temperatures. The sample size is 15 × 6 × 2 mm^3. To avoid demagnetization, the magnetic field was applied along the length direction. Magnetic field induced strains both parallel and perpendicular to the field direction (defined as $\lambda_{//}$ and $\lambda_{\perp}$, respectively) were measured. High-resolution S-XRD measurements were carried out to detect the tiny lattice distortion and to determine the crystal symmetry. Zero-field S-XRD experiments were performed at the 11-ID-C beam line of the Advanced Photon Source (APS), Argonne National Laboratory (photon energy = 111 keV). Wavelength of the x-ray is 0.11725 Å. All the samples for S-XRD were in powder form. The powders were carefully milled under the protection of ethanol. The powders were sieved using a 400 mesh/$inch^2$ sifter and sealed into quartz capillaries with inner diameter of 0.02 inch. The capillary was rotated during the measurement

to reduce the preferred orientation effect and to average the intensity. During the S-XRD measurement, the sample temperature was controlled by a Cryo-stream N_2 gas blower (from 90 to 300 K).

III. RESULTS

Fig. 1 shows the magnetic phase diagram of pseudo-binary $(DyCo_2)_{1-x}(DyFe_2)_x$ system. It is determined by temperature-dependent magnetostrictions (Figs. 2 and 3), temperature-dependent magnetizations (Fig. 4), temperature-dependent AC susceptibility (Fig. 5) and the *in-situ* synchrotron XRD (Fig. 6). This system has a common paramagnetic cubic phase at high temperature, which distorts into a tetragonal phase with $c/a > 1$ (T2) when cooling slightly below T_C, followed by a two-phase regime (one tetragonal phase with $c/a > 1$ and the other with $c/a < 1$), and finally transforms into another tetragonal phase with $c/a < 1$ (T1) at low temperatures. Following the concept of ferromagnetic MPB separating two ferromagnetic phases of differed structure in the formerly reported $TbCo_2$-$DyCo_2$, $TbFe_2$-$DyFe_2$, $TbCo_2$-$GdCo_2$, and $TbFe_2$-$GdFe_2$ systems [23-25, 30-34], the broaden regime that separates the T1 and T2 in the present $DyCo_2$-$DyFe_2$ system can also be deemed as a new type of ferromagnetic MPB.

The temperature-dependent magnetostrictions $\lambda_{//}$ and $\lambda_{\perp}$ for the samples with x = 0.08, 0.16, and 0.24 are shown in Figs. 2 and 3, respectively. Above MPB (for instance, x = 0.08 at 250 K), "□" shape $\lambda_{//}$ - H curve is observed, like that for the right terminal compound $DyFe_2$ [2, 6]. It means that the sample elongates along the parallel direction when increasing the magnetic field and the T2 phase has an intrinsic positive $\lambda_{//s}$. Below MPB (for instance, x = 0.08 at 50 K and x = 0.24 at 140 K), "□" shape $\lambda_{//}$ - H curve is observed, like that for the left terminal compound $DyCo_2$ [2, 6, 37]. It means that the sample contracts along the parallel direction when increasing the magnetic field and the T1 phase has an intrinsic negative $\lambda_{//s}$. Within the MPB regime, "W" shape $\lambda_{//}$ - H curve is observed, meaning that the sample

contracts at lower external fields and elongates at higher external fields. As denoted in Fig. 2(a), absolute value of the $\lambda_{//}$ reaches maximum at a critical magnetic field H_{cr} (not the coercivity H_c). At fields above H_{cr}, the $\lambda_{//}$ starts to go upwards. The "W" shaped magnetostriction curve can be regarded as a combination of "□" and "□" shaped curves, resulting from the offset between the coexisting T1 and T2 phases with opposite $\lambda_{//s}$. As shown in Fig. 3, the system exhibits "V" shape $\lambda_{\perp}$- H curve for T1 phase (x = 0.08 at 50 K, Fig. 3a) and "M" shape $\lambda_{\perp}$- H curve within the MPB regime (x = 0.16 at 160 K, Fig. 3b). It then excludes the possible magnetic-field-induced volume change effect. Such sign-changed-magnetostriction effect is similar to that observed in dual-phase Fe-Ga alloy [38], for which the net effect between the body-centered-cubic (bcc) phase with weaker magnetocrystalline anisotropy and intrinsic positive $\lambda_{//s}$ and the face-centered-cubic (fcc) phase with stronger magnetocrystalline anisotropy and intrinsic negative $\lambda_{//s}$ results in "M" shape $\lambda_{//}$ - H curve. Consequently, the initial contraction and the following elongation along the field direction suggest that the T1 phase has weaker magnetocrystalline than the T2 phase within the MPB regime.

The high temperature paramagnetic cubic parent phase is determined by the zero magnetization and susceptibility above T_C (Figs. 4 and 5) and the unsplitted {222} and {008} reflections (x = 0.08 at 300 K, Fig. 6a). It is noted that the tetragonal distortion of a cubic structure produces splitting in the {00l} reflections rather than the {hhh} ones due to the inequivalent lattice spacing among (100), (010) and (001). With increased Fe content, the unsplitted {222} peak shifts towards smaller Bragg diffraction angles, revealing increased d_{222}-spacing. Moreover, T_C also increases with Fe content from 140 K for the $DyCo_2$ to 264 K for x = 0.08, 383 K for x = 0.16, and 484 K for x = 0.24 (Fig. 4). This enhancement is consistent with the nature of the magnetic moments of 3d sublattice of RFe$_2$ and RCo$_2$ systems [2, 6]. It also indicates that the Fe atoms partially substitute for the Co in the RT_2 lattice. Below T_C, the

system undergoes an extra ferromagnetic → ferromagnetic transition (as reflected by the broaden peak in χ'-T curves in Figs. 5b and 5c), which has not been observed in either $DyCo_2$ or $DyFe_2$. Similar susceptibility peak has also been observed in the formerly reported ferromagnetic MPBs, for which the ferromagnetic → ferromagnetic transition is also a crystallographic phase transition associated with lattice softening [23, 30]. As the two terminals that form a MPB have strongly temperature-dependent magnetocrystalline anisotropies, two tetragonal phases then coexist over a broad temperature interval. For the present $DyCo_2$-$DyFe_2$ system, the continuous change in χ' is also across a broadening temperature range, which is more apparent for the compounds with x = 0.16 and x = 0.24 than that for the compound with x = 0.08 (Fig. 5).

The phase constituents within the MPB regime are also evaluated by *in situ* S-XRD data. For the compound with x = 0.08 at 90 K (far below T_C), the asymmetric (800) reflection splits into two peaks, as shown in Fig. 6(a). Fitted by the Gaussian function, one represents the (800)/(080) reflections (the blue profile) and the other is the (008) reflection (the green profile), and the area ratio between them is ~2:1. The appearance of the reflection with smaller area at larger Bragg angle indicates a tetragonal distortion with $c < a$, which is consistent with the lattice distortion for the parent terminal $DyCo_2$. Within the MPB regime (Fig. 5), the (800) reflection for the compounds with x = 0.16 and 0.24 splits into three peaks (e.g. x = 0.08 at 90 K, as in Fig. 6b), similar to that for an orthorhombic structure. No splitting however, is observed for the {222} reflection, excluding the orthorhombic structure. In fact, it reflects the coexistence of two tetragonal phases (green profile for T1 phase and orange profile for T2 phase) with opposite lattice distortion along the c axis, since one of the additional weak reflections lies at the lower Bragg angle side and the other at the higher side. The weak splitting for the $(008)_{T2}$ is consistent with the lattice distortion for $DyFe_2$ with $c > a$ [6]. Consequently, the S-XRD data directly reveals that the ferromagnetic MPB in $DyCo_2$-$DyFe_2$ system contains

two tetragonal phases. Note that with decreased temperature, intensity for the $(008)_{T2}$ reflection decreases, accompanied with increased intensity for the $(008)_{T1}$ reflection, suggesting that fraction of T1 phase increases at the expense of that of the T2 phase upon cooling.

Fig. 7 illustrates the magnetization hysteresis loops for $DyCo_2$-$DyFe_2$ samples with x = 0.08, 0.16, and 0.24, respectively. At all measured temperatures, the magnetization is nearly saturated at the maximum measurement field of 20 kOe. When the sample contains single phase (e.g. x = 0.08 at 50 K), the magnetostriction $\lambda_{//}$ is also nearly saturated. However, the magnetostrictions for the MPB regime are not saturated even at 20 kOe. At different temperatures, the magnetizations increase as the field strength is enhanced although the magnetostriction sign changes within the MPB regime. It is noted that within the MPB regime, both the critical field H_{cr} and the magnetostriction $\lambda_{//cr}$ increase with decreased temperature (Fig. 8), indicating that a much larger field is required to completely reorient the variants of T1 phase due to its enhanced magnetocrystalline anisotropy and the enlarged volume fraction. At the bottom of Fig. 8 (a), $\lambda_{//20kOe}$ for the compound with x = 0.08 indeed reach nearly zero at 200 K, above which it is positive and below which it becomes negative. It reflects the net effect of the average tetragonality, which transforms from $c/a > 1$ to $c/a = 1$ and to $c/a < 1$ with decreased temperature. The data in Figs. 8(b) and (c) for the compounds with x = 0.16 and 0.24 also show similar temperature dependences of magnetostriction and critical field H_{cr}.

The corresponding temperature dependences of coercivity H_C, remanence M_r and magnetization M_{20kOe} are also summarized in Fig. 8. All of them rise with the decrement of temperature for these three samples (x = 0.08, 0.16 and 0.24). The gradual magnetization enhancement is due to the enhanced magnetic ordering degree upon cooling. The coercivity and remanence however, are not minimized at MPB, implying that no magnetocrystalline anisotropy compensation occurs for the present $DyCo_2$-$DyFe_2$ system, unlike the formerly reported MPBs in $TbCo_2$-$DyCo_2$, $TbFe_2$-$DyFe_2$, $TbCo_2$-$GdCo_2$, and $TbFe_2$-$GdFe_2$ systems.

Actually, for these systems, the sign of magnetocrystalline anisotropy constant K_1 for the rhombohedral phase ($TbFe_2$ or $TbCo_2$ below T_C) is opposite to that for the tetragonal phase (e.g. $DyFe_2$ or $DyCo_2$ below T_C). Their coexistence gives rise to magnetocrystalline anisotropy compensation at a proper fraction and a certain temperature. For the present $DyCo_2$-$DyFe_2$ system, both T1 and T2 phases possess [001] easy axis and have the same sign in K_1 ($K_1 > 0$) [1-3], hence no anisotropy compensation can be reached within the MPB regime.

IV. DISCUSSION

The noncubic crystal symmetry of the ferromagnetic phase demonstrates that a magnetic domain is also a ferroelastic or crystallographic variant [37, 39]. *In situ* S-XRD data taken from the $Tb_{0.3}Dy_{0.7}Fe_2$ and $DyCo_2$ under different magnetic fields reveal that switching of magnetic domains by magnetic field is also switching of the ferroelastic variants. In principle, for a tetragonal phase, there are three kinds of variants generated from one cubic crystal grain, corresponding to contraction or elongation of the $[001]_C$, $[010]_C$, and $[100]_C$ axes, respectively. The growth of preferred variant is a way for magnetization reorientation under the external fields, leading to the macroscopic magnetostriction. For either T1 or T2 polycrystalline samples, only the variant with easy-axis parallel to the field direction grows via magnetization reorientation, generating either negative or positive $\lambda_{//}$ (Figs. 9a and 9b). Within the MPB regime, the magnetostriction mechanism is schematically shown in Fig. 9(c). There are two types of tetragonal variants with opposite lattice distortion units. Under low magnetic fields, the crystal contracts along the field direction as the T1 variants preferably switch due to their smaller magnetocrystalline anisotropy rather than those for the T2, and exhibits the "□"-shaped $\lambda_{//}$ - H curve ("V"-shaped $\lambda_{\perp}$- H curve). At higher fields, it exhibits positive parallel magnetostriction ($\Delta L > 0$) due to the reorientation of T2 variants. Similar preferable domain switches have been observed in bi-phase Fe-Ga alloys by in-situ Lorentz TEM [38].

The highly temperature-dependent magnetostriction is related to the fraction of the T1 and T2 phases and the corresponding magnetocrystalline anisotropy energy for each phase ($K_U \approx M_s H_a/2$, where M_s is the saturation magnetization and H_a is the anisotropic field). The K_U is highly dependent on both temperature and composition. According to the Bloch $T^{3/2}$ law [40-42], $K_U \approx K_1$ for a cubic ferromagnet with <001> easy axis, and below T_C it is given by

$$K_1(T) = K_1(0)[1 - (T/T_C)^p]^n \quad (1)$$

where $K_1(T)$ and $K_1(0)$ is the magnetocrystalline anisotropy constant at temperature T and 0 K, respectively. The exponent p is close to 3/2, while n is a symmetry-related constant. Since both the parent $DyCo_2$ and $DyFe_2$ are tetragonal below T_C, the difference in p and n between T1 and T2 phase can be ignored. As $DyCo_2$ (T_C =140 K) exhibits a much lower T_C than $DyFe_2$ (T_C = 635 K), the T1 phase then possesses a smaller K_1 than that of the T2 phase at a certain temperature slightly below T_C. Consequently, when the composition is fixed, the initial negative $\lambda_{//}$ stems from the primary magnetization reorientation of T1 phase in lower external fields (Figs. 2 and 8). Because the magnetocrystalline anisotropy energies for both tetragonal phases will be enhanced upon cooling, the critical field H_{cr} at which the magnetostriction goes upwards becomes larger when cooling to lower temperatures (Figs. 2 and 8). When the magnetocrystalline anisotropy energy and the volume fraction of T1 phase become far stronger or larger than those for the T2 phase, the $\lambda_{//}$ - H curve exhibits a "□" shape rather than retaining the "W" shape. It is also noted that the T_C increases with the increment of Fe content, meaning that the K_U is different for the samples with x = 0.08, 0.16 and 0.24 at the same temperature. We take the curves measured at 300 K as references, the sample with x = 0.16 contains a smaller volume fraction of T1 variants and exhibiting weaker magnetocrystalline anisotropy compared to the sample with x = 0.24. It results in three different magnetostriction behaviors (Fig. 2), including smaller negative $\lambda_{//}$ (due to the switch of T1 variants), lower critical field at

which $\lambda_{//}$ sign changes and easily saturated positive $\lambda_{//}$ (due to the switch of T2 variants) for x = 0.16.

The above findings are of significant importance. Firstly, it brings new insights into the ferromagnetic MPB theory of pseudobinary RT_2 compounds. Unlike the formerly-reported pseudobinary $TbCo_2$-$DyCo_2$, $TbFe_2$-$DyFe_2$, $TbCo_2$-$GdCo_2$, and $TbFe_2$-$GdFe_2$ systems with a tetragonal and a rhombohedral terminals [23-25, 30-34], for which MPB results in anisotropy compensation, the present MPB for $DyCo_2$-$DyFe_2$ with two tetragonal terminals does not result in anisotropy compensation due to the same sign K_1. In addition, the present MPB has a much broadening temperature range than previously reported ones. Since the magnetocrystalline anisotropy energy that governs the formation of ferromagnetic MPB is closely related to T_C [24], the wide MPB temperature regime of the present system is due to the large difference in T_C between the two terminals, as summarized in Table 1. Such difference (395 K) in T_C-$DyFe_2$ and T_C-$DyCo_2$ is over 3 times larger than that for the $TbCo_2$-$DyCo_2$, $TbFe_2$-$DyFe_2$, $TbCo_2$-$GdCo_2$, and $TbFe_2$-$GdFe_2$, e.g. the difference between T_C-$TbFe_2$ and T_C-$DyFe_2$ is only 62 K [2]. Secondly, it provides deeper understanding of the magnetostrictive responses of ferromagnetic MPBs. Different magnetostrictive responses among the three types of ferromagnetic MPB are summarized in Table 1 and Fig.10. Both the sign of λ_s and K_1 for the two terminals determine their magnetostriction responses. Since the former two types have compensated anisotropy due to the opposite K_1, the enhanced magnetostriction for type-I MPB is resulted from the simultaneous switching of both tetragonal and rhombohedral phases with positive λ_s, while the weakened magnetostriction for the type-II MPB is due to the simultaneous switching of both tetragonal and rhombohedral phases with the opposite λ_s. The sign-changed-magnetostriction for the type-III MPB, however, arises from the preferable domain switches between the two coexisting tetragonal phases with inequivalent magnetocrystalline anisotropy and opposite λ_s. Finally, the

sign-changed-magnetostriction effect may facilitate novel engineering applications. The linear magnetostriction of single phase ferromagnets, including pure metals such as Fe or Ni, alloys such as Fe-Co, and intermetallic compounds including $DyFe_2$ or $DyCo_2$, is either negative or positive with increased magnetic field strength, allowing only monotonous control. Analogous to the present MPB in $DyCo_2$-$DyFe_2$, the sign-changed-magnetostriction ("*M*" type $\lambda_{//}$ - *H* curve) has also been obtained in a Fe-Ga composite [38]. Such materials with sign-changed-magnetostriction may output either one-dimensional contraction or elongation by tuning the field strength (bi-conditional control), without the requirement for stacked composites. In addition, as verified in the Fe-Ga composite containing BCC and FCC phases with opposite magnetostriction signs, stress-insensitive magnetic permeability and coercivity have been obtained due to the compensation of stress-induced extra anisotropies [43]. Such appealing magnetic properties can also be achieved in the present $DyCo_2$-$DyFe_2$. It may also serve as a soft magnet for potential applications under high stress.

V. CONCLUSIONS

In summary, a new type of ferromagnetic morphotropic phase boundary with sign-changed-magnetostriction effect has been found in the $DyCo_2$-$DyFe_2$ system. Unlike the enhanced or weakened magnetostriction effects of the formerly reported MPBs separating a tetragonal phase and a rhombohedral phase, the sign-changed-magnetostriction effect of the present MPB is due to the hybrid of strain behaviors from two tetragonal phases with intrinsic magnetostrictions of opposite sign. It is a net result from the domain switches of these two coexisting components with different magnetocrystalline anisotropies. Besides, the present MPB does not possess minimized coercivity since the two tetragonal phases have the same sign in magnetocrystalline anisotropy constant. It suggests that proper placing two end terminals with different structures and intrinsic magnetic properties at MPB enables desirable engineering properties.

ACKNOWLEDGEMENTS

This work was supported by the National Natural Science Foundation of China (Grant Nos. 51622104, 51871174, 51431007, 51831006, 51471125, 51471127 and 51601140), the Young Talent Support Plans of Shaanxi province and XJTU, the Program for Changjiang Scholars and Innovative Research Team in University (IRT-17R85), and the Fundamental Research Funds for the Central Universities. We thank Dr. Yang Ren of Argonne National Laboratory for the help of using resources of the Advanced Photon Source, a U.S. Department of Energy (DOE) Office of Science User Facility operated for the DOE Office of science (Contract No. DE-AC02-06CH11357).

References

[1] K.H.J. Buschow, Rep. Prog. Phys. **40**, 1179 (1977).

[2] A.E. Clark, Ferromagnetic Materials, North-Holland, Amsterdam, (1980).

[3] M.D. Kuz'min and A.M. Tishin, Handbook of Magnetic Materials **17**, 149 (2007).

[4] J.H. Liu, C.B. Jiang, and H.B. Xu, Sci. China Ser. E: Technol. Sci. **55**, 1319 (2012).

[5] W.J. Ren and Z.D. Zhang, Chin. Phys. B **22**, 077507 (2013).

[6] E. Gratz, A.S. Markosyan, J. Phys. Condens. Matter **13**, R385 (2001).

[7] Z.W. Ouyang, F.W. Wang, Q. Huang, W.F. Liu, Y.G. Xiao, J.W. Lynn, J.K. Liang, and G.H. Rao, Phys. Rev. B **71**, 064405 (2005).

[8] Niraj K. Singh, S. Agarwal, K.G. Suresh, R. Nirmala, A.K. Nigam, S.K. Malik, Phys. Rev. B **72**, 014452 (2005).

[9] R. Ranchal, V. Gutiérrez-Díez, and V. González Martín, Acta Mater. **60**, 1840 (2012).

[10] Z. Śniadecki, N. Pierunek, B. Idzikowski, B. Wasilewski, M. Werwiński, U. K. Rößler, and Yu. Ivanisenko, Phys. Rev. B **98**, 094418 (2018).

[11] A. Murtaza, S. Yang, T.Y. Chang, A. Ghani, M.T. Khan, R. Zhang, C. Zhou, X.P. Song, M. Suchomel, and Y. Ren, Phys. Rev. B **97**, 104410 (2018).

[12] U. Atzmony, M.P. Dariel, E.R. Bauminger, D. Lebenbaum, I. Nowik, and S. Ofer, Phys. Rev. Lett. **28**, 244 (1972).

[13] U. Atzmony, M.P. Dariel, and G. Dublon, Phys. Rev. B **15**, 3565 (1977).

[14] J. Cullen and A.E. Clark, Phys. Rev. B **15**, 4510 (1977).

[15] A.E. Clark, J.P. Teter, and O.D. McMasters, J. Appl. Phys. **63**, 3910 (1988).

[16] G.H. Wu, X.G. Zhao, J.H. Wang, J.Y. Li, K.C. Jia and W.S. Zhan, Appl. Phys. Lett. **67**, 2005 (1995).

[17] Y.M. Pei, D.N. Fang, and X. Feng, Appl. Phys. Lett. **90**, 182505 (2007).

[18] C.S. Zhang, T.Y. Ma, and G.A. Sun, Appl. Phys. Lett. **110**, 062403 (2017).

[19] D.C. Jiles, Acta Mater. **51**, 5907 (2003).

[20] T.L. Zhang, C.B. Jiang, L.H. Xu, Smart Mater. Struct. **14**, N38 (2005).

[21] A.G. Olabi and A. Grunwald, Mater. Des. **29**, 469 (2008).

[22] G. Lanza, G. Breglio, M. Giordano, A. Gaddi, S. Buontempo, and A. Cusano, Sens. Actuators A **172**, 420 (2011).

[23] S. Yang, H.X. Bao, C. Zhou, Y. Wang, X.B. Ren, Y. Matsushita, Y. Katsuya, M. Tanaka, K. Kobayashi, X.P. Song, and J.R. Gao, Phys. Rev. Lett. **104**, 197201 (2010).

[24] R. Bergstrom Jr., M. Wuttig, J. Cullen, P. Zavalij, R. Briber, C. Dennis, V.O. Garlea, and M. Laver, Phys. Rev. Lett. **111**, 017203 (2013).

[25] Z.H. Nie, S. Yang, Y.D. Wang, Z.L. Wan, D.M. Liu, Y. Ren, T.Y. Chang, and R. Zhang, J. Alloys Compd. **658**, 372 (2016).

[26] B. Jaffe, W.R. Cook, and H. Jaffe, Piezoelectric Ceramics, Academic Press, New York, 1971.

[27] Y. Saito, H. Takao, T. Tani, T. Nonoyama, K. Takatori, T. Homma, T. Nagaya, and M. Nakamura, Nature **432**, 84 (2004).

[28] M. Ahart, M. Somayazulu, R.E. Cohen, P. Ganesh, P. Dera, H.K. Mao, R.J. Hemley, Y. Ren, P. Liermann, and Z. Wu, Nature **451**, 545 (2008).

[29] W.F. Liu and X.B. Ren, Phys. Rev. Lett. **103**, 257602 (2009).

[30] C. Zhou, S. Ren, H. Bao, S. Yang, Y.G. Yao, Y.C. Ji, X.B. Ren, Y. Matsushita, Y. Katsuya, M. Tanaka, and K. Kobayashi, Phys. Rev. B **89**, 100101(R) (2014).

[31] M. Adil, S. Yang, M. Mi, C. Zhou, J.Q. Wang, R. Zhang, X.Q. Liao, Y. Wang, X.B. Ren, X.P. Song, and Y. Ren, Appl. Phys. Lett. **106**, 132403 (2015).

[32] M. Adil, S. Yang, C. Zhou, T.Y. Chang, K.Y. Chen, F.H. Tian, X.P. Song, M. R. Suchomel, and Y. Ren, Appl. Phys. Lett. **109**, 052904 (2016).

[33] T.Y. Ma, X.L. Liu, X.W. Pan, X. Li, Y.Z. Jiang, M. Yan, H.Y. Li, M.X. Fang, and X. B. Ren, Appl. Phys. Lett. **105**, 192407 (2014).

[34] C. C. Hu, T. N. Yang, H. B. Huang, J. M. Hu, J. J. Wang, Y. G. Shi, D. N. Shi, and L. Q. Chen, Appl. Phys. Lett. **108**, 141908 (2016).

[35] D. Bloch and R. Lemaire, Phys. Rev. B **2**, 2648 (1970).

[36] E. Burzo, Phys. Rev. B **17**, 1414 (1978).

[37] S. Yang and X.B. Ren, Phys. Rev. B **77**, 014407 (2008).

[38] J.M. Gou, X.L. Liu, K.Y. Wu, Y. Wang, S.S. Hu, H. Zhao, A.D. Xiao, T.Y. Ma, and M. Yan, Appl. Phys. Lett. **109**, 082404 (2016).

[39] S. Yang, X.B. Ren, and X.P. Song, Phys. Rev. B **78**, 1742 (2008).

[40] F. Bloch, Zur Theorie des Ferromagnetismus, Z. Phys. **61**, 206 (1930).

[41] S. Longhi, Phys. Rev. Lett. **103**, 123601 (2009).

[42] C. Zener, Phys. Rev. **96**, 1335 (1954).

[43] J.M. Gou, X.L. Liu, C.S. Zhang, G.A. Sun, Y.N. Shi, J. Wang, H.X. Chen, T.Y. Ma, and X.B. Ren, Phys. Rev. Mater. **2**, 114406 (2018).

Figure Captions

FIG. 1 Magnetic phase diagrams for pseudobinary $DyCo_2$-$DyFe_2$. Red dots are Curie temperatures T_C determined from the *M-T* curves, and star symbols mark the transitions recognized from χ'-*T* curves, crystal symmetry at different magnetic states is determined by synchrotron XRD data. Schematic λ – H curves refer to the magnetostriction parallel to the field direction. (Single column)

FIG. 2 Parallel magnetostrictions ($\lambda_{//}$) by in-situ cooling the $(DyCo_2)_{1-x}(DyFe_2)_x$ samples to different temperatures. (a) x = 0.08, (b) x = 0.16, and (c) x = 0.24. H_{cr} is the critical field at which contraction changes into elongation, λ_{cr} is the corresponding negative magnetostriction magnitude. (Double column)

FIG. 3 Perpendicular magnetostrictions ($\lambda_{\perp}$) for $(DyCo_2)_{1-x}(DyFe_2)_x$ samples at different temperatures. (a) x = 0.08 and (b) x = 0.16. (Single column)

FIG. 4 Temperature dependence of magnetization for $(DyCo_2)_{1-x}(DyFe_2)_x$ samples. (a) x = 0.08, (b) x = 0.16, and (c) x = 0.24. (Single column)

FIG. 5 Temperature dependence of AC susceptibility χ' for $(DyCo_2)_{1-x}(DyFe_2)_x$ samples. (a) x = 0.08, (b) x = 0.16, and (c) x = 0.24. The star symbols denote the MPB regime. (Single column)

FIG. 6 *In-situ* cooling HR-SXRD data for $(DyCo_2)_{1-x}(DyFe_2)_x$ powder samples with x = 0.08 (a), 0.16 (b), and 0.24 (c), where the enlarged reflections (222) and (800) are shown in each bottom. The green line corresponds to the tetragonal splitting of T1 ($c/a > 1$) and orange to T2 ($c/a < 1$). (Double column)

FIG. 7 Isothermal *M* - *H* hysteresis loops for $(DyCo_2)_{1-x}(DyFe_2)_x$ measured upon *in-situ* cooling the sample to different temperatures at zero field. (a) x = 0.08, (b) x = 0.16, and (c) x = 0.24. (Double column)

FIG. 8 Temperature dependences of the coercivity H_c, saturation magnetization M_s,

remanence M_r, the critical field H_{cr} at which strain signal changes, the parallel magnetostriction magnitude at H_{cr}, and the net parallel magnetostriction at 20 kOe, λ_{20kOe} for $(DyCo_2)_{1-x}(DyFe_2)_x$ compounds with x = 0.08 (a), 0.16 (b), and 0.24 (c). (Double column)

FIG. 9 Schematically mesoscopic explanations for magnetostriction due to the switching of the tetragonal ferromagnetic (ferroelastic) variants with different tetragonalities. The rectangles T1 represents the tetragonality $c/a < 1$, T2 represents tetragonality $c/a > 1$. ΔL is the parallel magnetostriction under the magnetic field H. (a) T1 phase, (b) T2 phase, (c) coexistence of T1 and T2 phases within MPB regime. (Double column)

FIG. 10 Comparison of magnetostriction in three types of ferromagnetic MPBs obtained in pseudobinary RT_2 compounds. (a) Type-I MPB with enhanced magnetostriction, (b) Type-II MPB with compensated magnetostriction, and (c) Type-III MPB with sign-changed magnetostriction. The parallel magnetostriction curves in (a) are obtained from $TbFe_2$-0.7$DyFe_2$ at different temperatures; the ones in (b) are obtained from $TbCo_2$-$GdCo_2$ with different compositions at room temperature (redrawn from ref. [30]); the ones in (c) are for $DyCo_2$-0.08$DyFe_2$ at different temperatures. (Double column)

Table 1 Magnetostrictive responses at MPB of pseudobinary RT_2 compounds.

	Type I		Type II		Type III	
	Terminal 1	Terminal 2	Terminal 1	Terminal 2	Terminal 1	Terminal 2
Compound	$TbFe_2$	$DyFe_2$	$TbCo_2$	$GdCo_2$	$DyFe_2$	$DyCo_2$
Symmetry [1]	R	T	R	T	T	T
Sign of λ_s	Positive	Positive	Positive	Negative	Positive	Negative
Sign of K_1	Negative	Positive	Negative	Positive	Positive	Positive
Magnetostriction at MPB	Enhanced		Weakened		Sign-changed	
T_C [2]	697 K	635 K	235 K	402 K	635 K	140 K
ΔT_C	62 K		167 K		395 K	

[1] R and T represent Rhombohedral and Tetragonal, respectively.

[2] T_C is cited from refs. [1, 2, 23, 30, 35, 36].

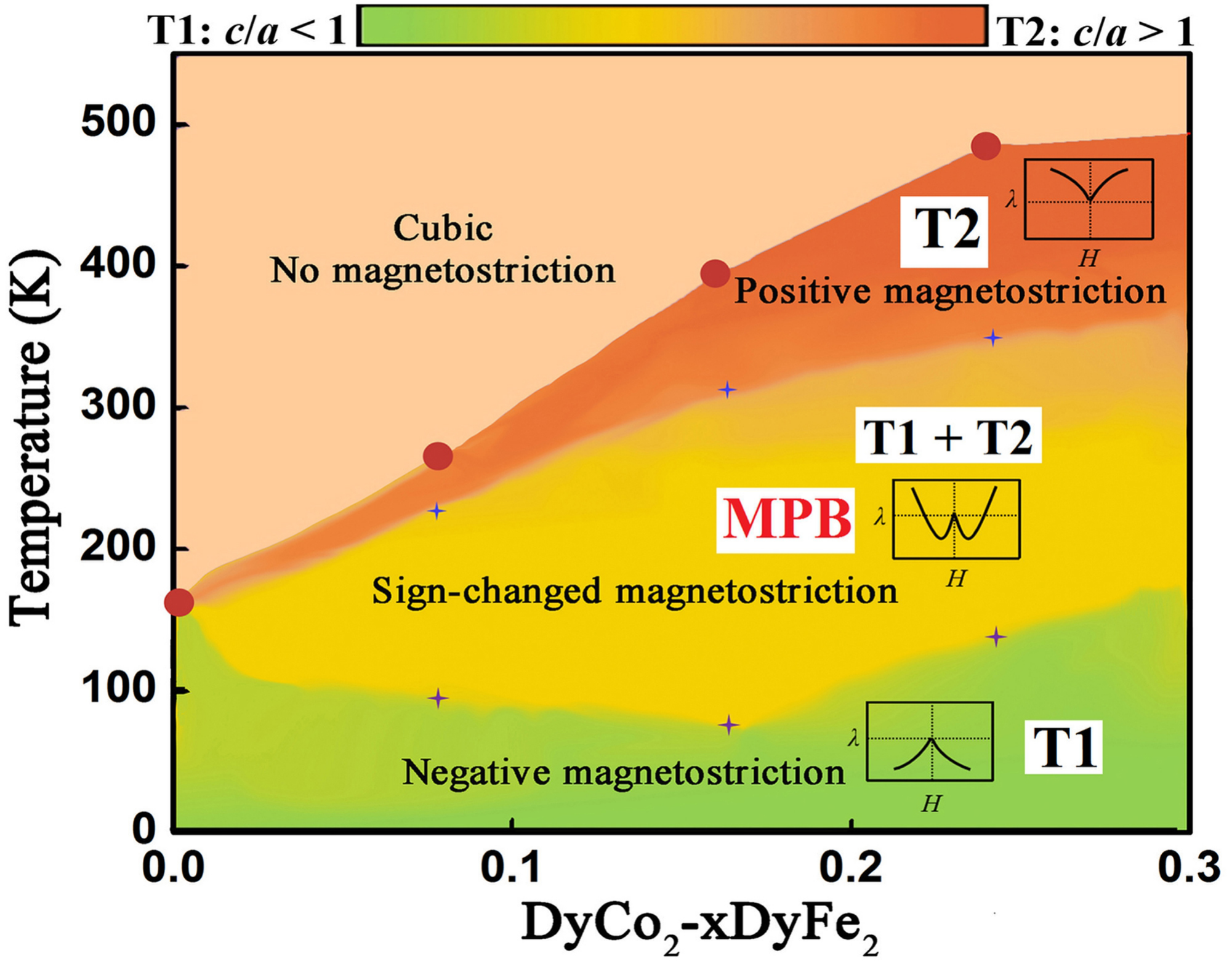
T1: c/a < 1
T2: c/a > 1
500
400
300
200
100
0
Temperature (K)
0.0
0.1
0.2
0.3
DyCo2-xDyFe2
Cubic
No magnetostriction
T2
Positive magnetostriction
T1 + T2
MPB
Sign-changed magnetostriction
T1
Negative magnetostriction
λ
H

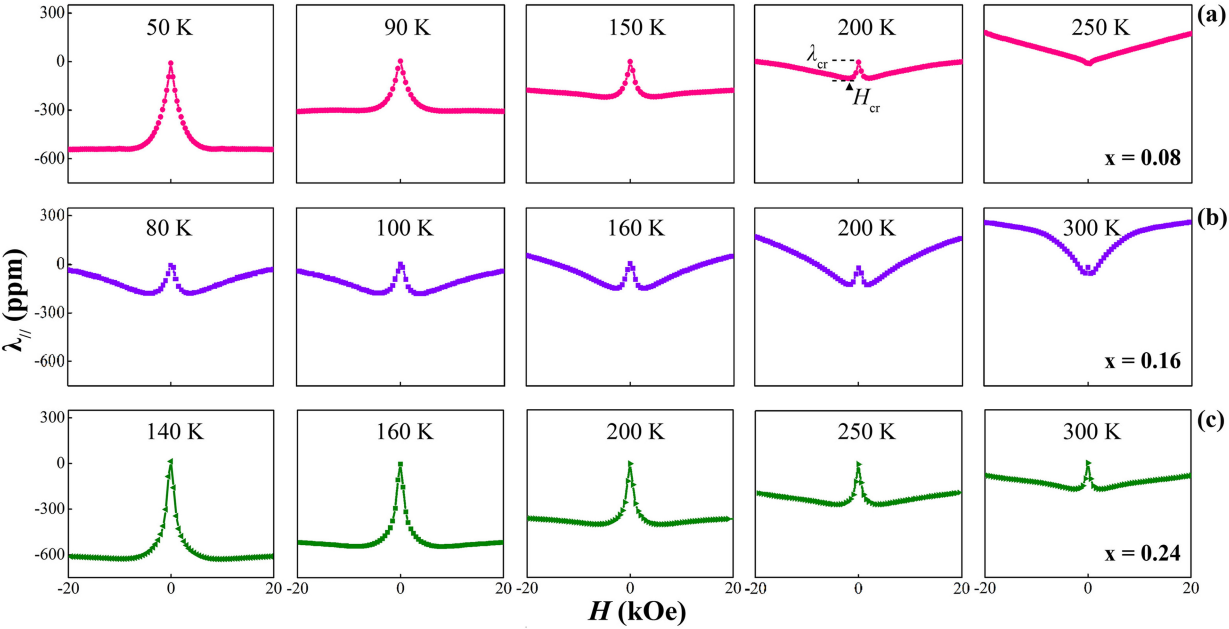
(a)
50 K
90 K
150 K
200 K
250 K
λ_{cr}
H_{cr}
x = 0.08
(b)
80 K
100 K
160 K
200 K
300 K
x = 0.16
(c)
140 K
160 K
200 K
250 K
300 K
x = 0.24
300
0
-300
-600
-20
0
20
$\lambda_{//}$ (ppm)
H (kOe)

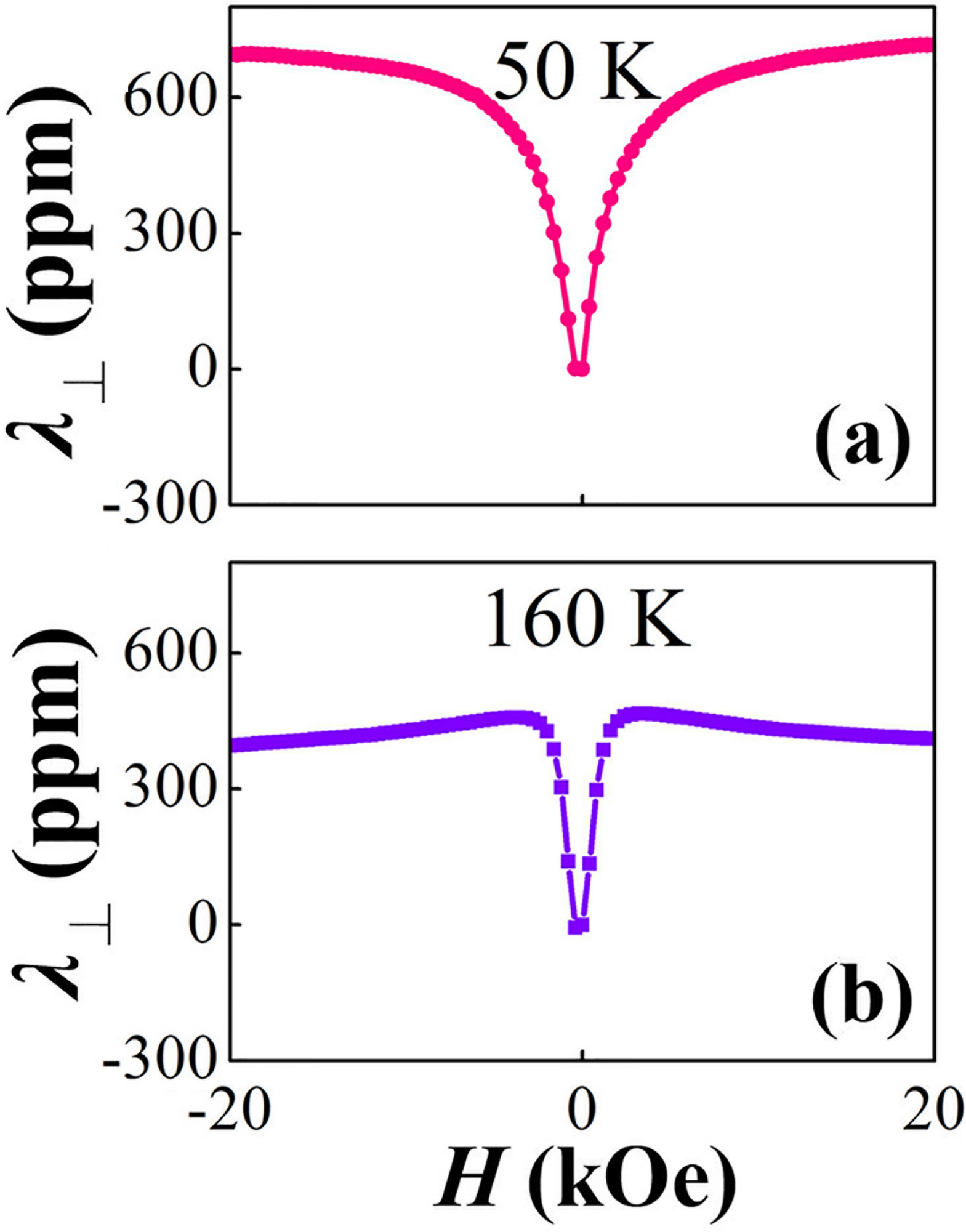
50 K
600
300
0
-300
$\lambda_\perp$ (ppm)
(a)
160 K
600
300
0
-300
$\lambda_\perp$ (ppm)
(b)
-20
0
20
H (kOe)

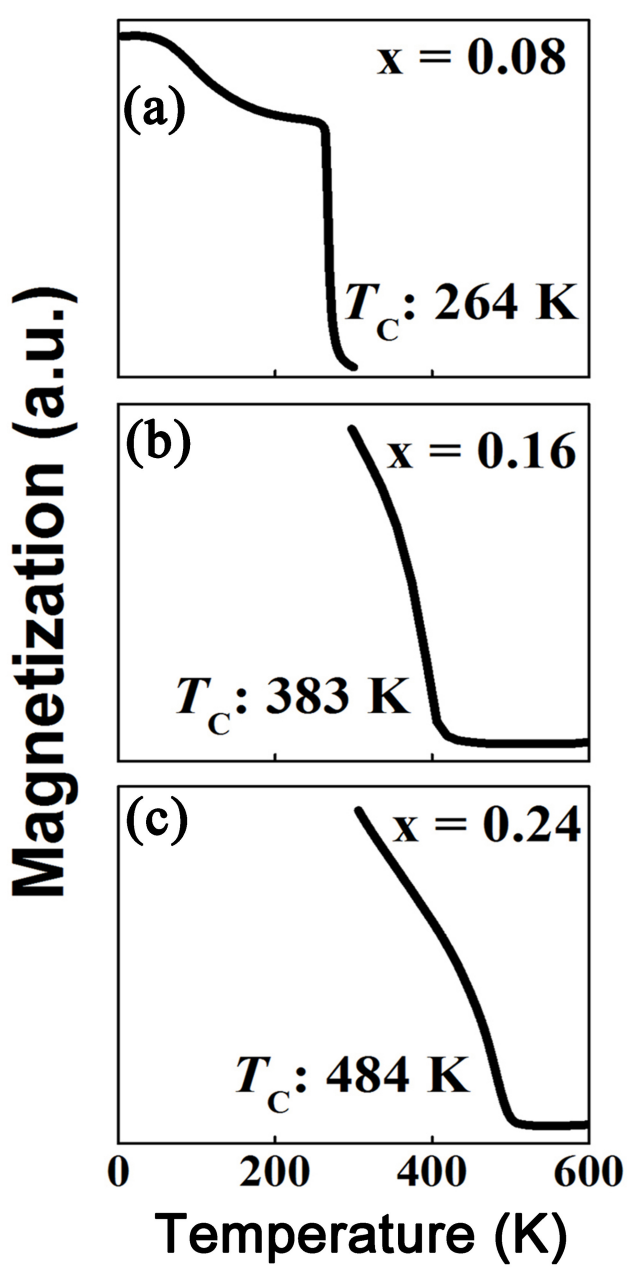
x = 0.08
(a)
T_C: 264 K
(b)
x = 0.16
T_C: 383 K
(c)
x = 0.24
T_C: 484 K
Magnetization (a.u.)
0
200
400
600
Temperature (K)

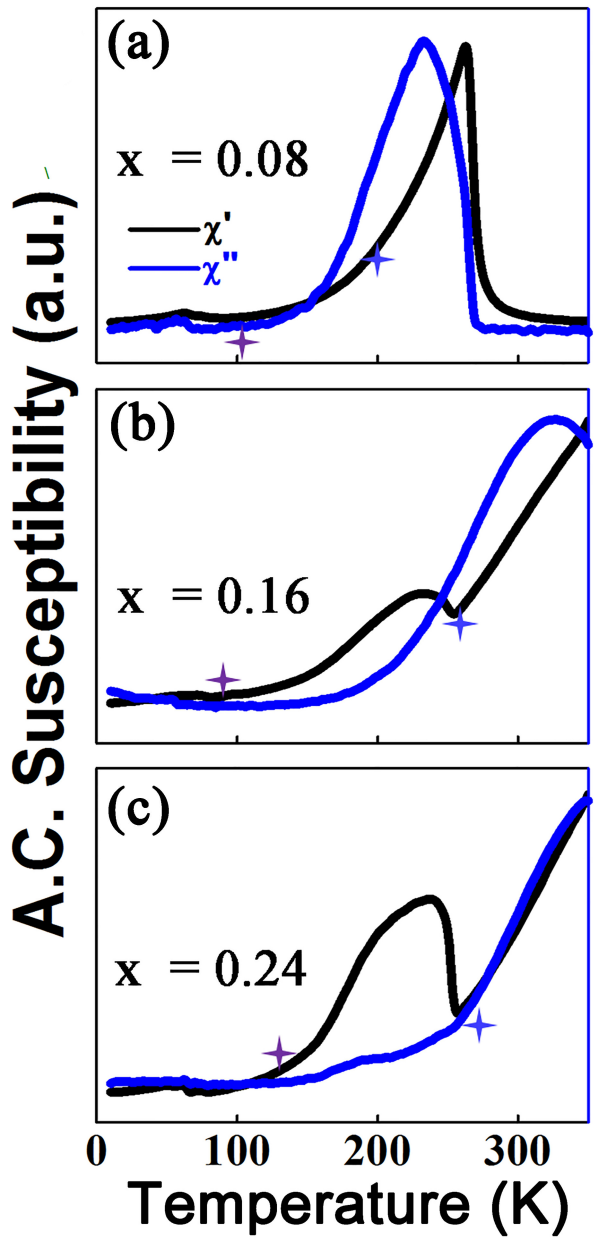
(a)
x = 0.08
χ'
χ''
(b)
x = 0.16
(c)
x = 0.24
A.C. Susceptibility (a.u.)
0
100
200
300
Temperature (K)

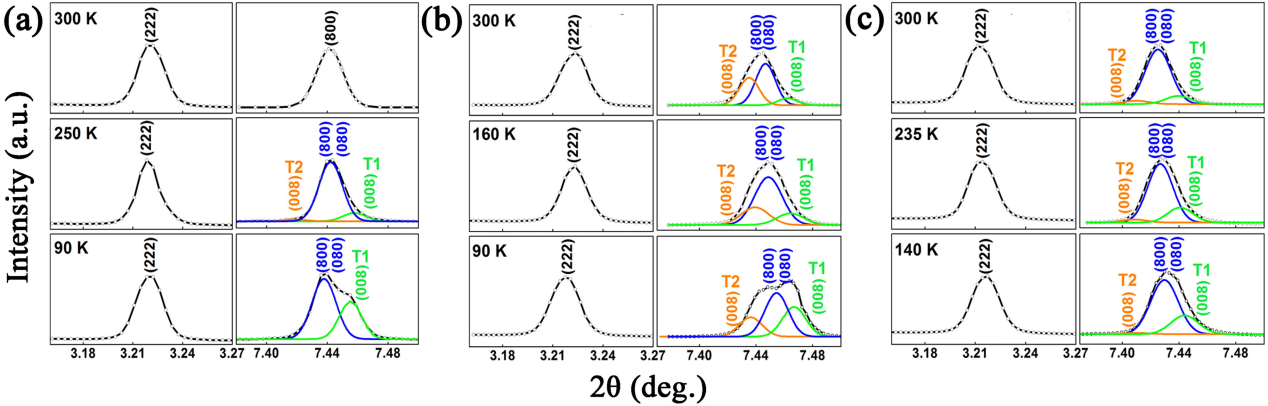
(a)
(b)
(c)
300 K
250 K
90 K
160 K
235 K
140 K
(222)
(800)
(800)
(080)
T2
(800)
T1
(008)
Intensity (a.u.)
3.18
3.21
3.24
3.27
7.40
7.44
7.48
2θ (deg.)

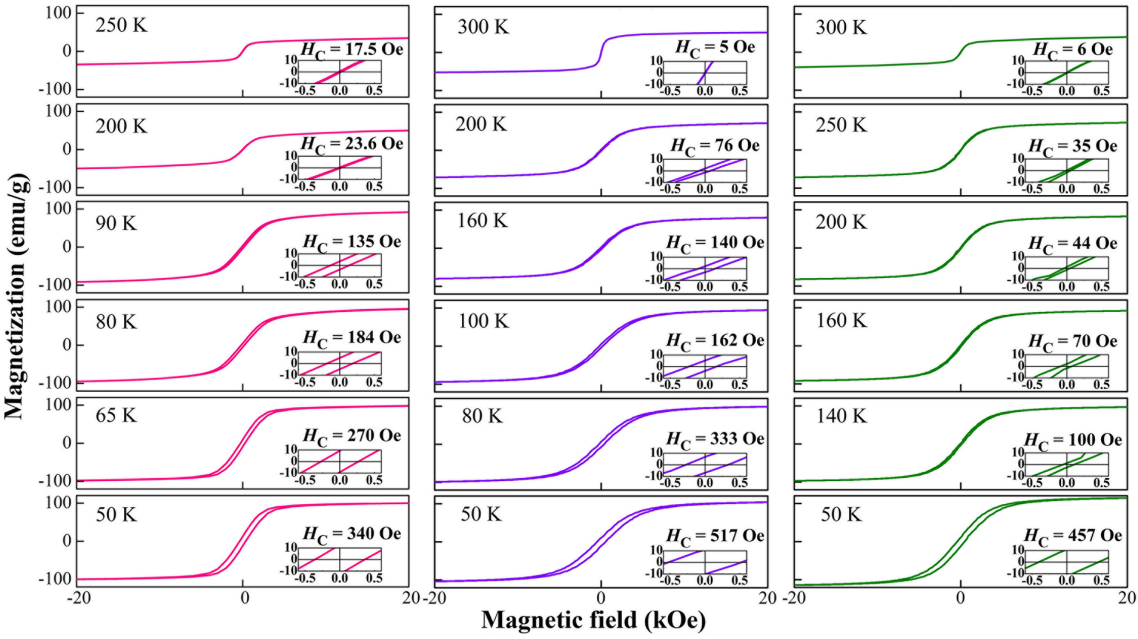
(a) x = 0.08
(b) x = 0.16
(c) x = 0.24
250 K
H_C = 17.5 Oe
200 K
H_C = 23.6 Oe
90 K
H_C = 135 Oe
80 K
H_C = 184 Oe
65 K
H_C = 270 Oe
50 K
H_C = 340 Oe
300 K
H_C = 5 Oe
200 K
H_C = 76 Oe
160 K
H_C = 140 Oe
100 K
H_C = 162 Oe
80 K
H_C = 333 Oe
50 K
H_C = 517 Oe
300 K
H_C = 6 Oe
250 K
H_C = 35 Oe
200 K
H_C = 44 Oe
160 K
H_C = 70 Oe
140 K
H_C = 100 Oe
50 K
H_C = 457 Oe
Magnetization (emu/g)
Magnetic field (kOe)

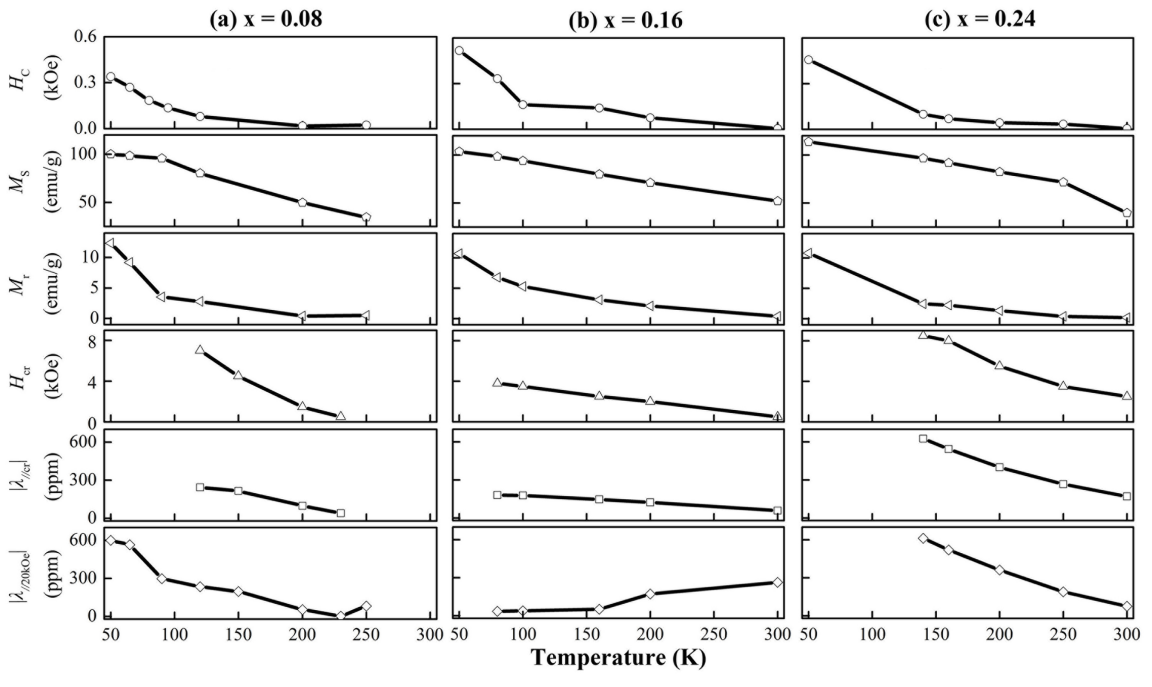
(a) x = 0.08
(b) x = 0.16
(c) x = 0.24
H_C (kOe)
M_S (emu/g)
M_r (emu/g)
H_{cr} (kOe)
$|\lambda_{//cr}|$ (ppm)
$|\lambda_{//20kOe}|$ (ppm)
Temperature (K)

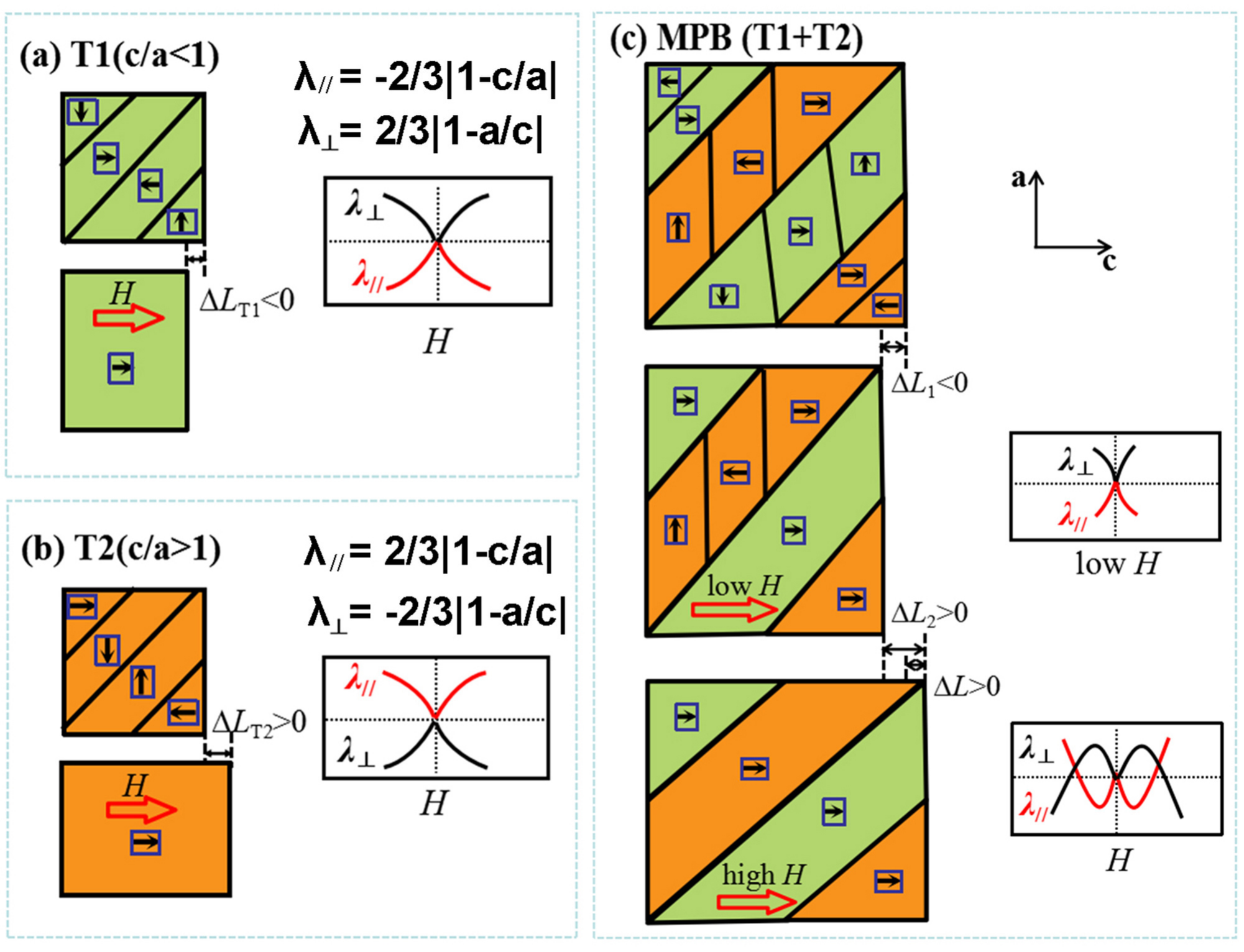
(a) T1(c/a<1)
λ// = -2/3|1-c/a|
λ⊥ = 2/3|1-a/c|
H
ΔL_T1<0
λ⊥
λ//
H
(b) T2(c/a>1)
λ// = 2/3|1-c/a|
λ⊥ = -2/3|1-a/c|
ΔL_T2>0
H
λ//
λ⊥
H
(c) MPB (T1+T2)
a
c
ΔL1<0
low H
ΔL2>0
ΔL>0
high H
λ⊥
λ//
low H
λ⊥
λ//
H

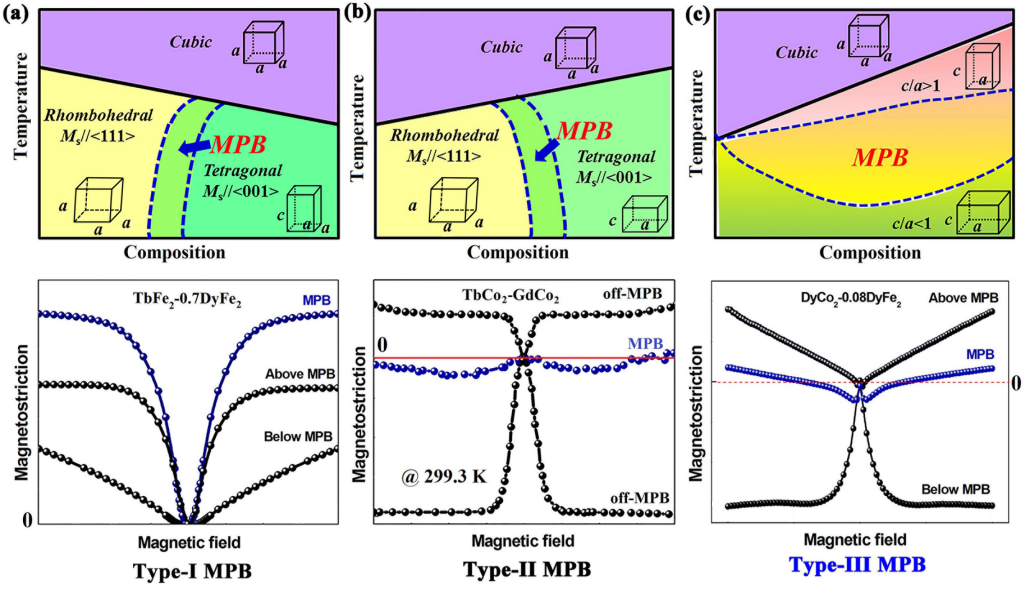
(a)
Cubic
Rhombohedral
M_s//<111>
MPB
Tetragonal
M_s//<001>
Temperature
Composition
(b)
Cubic
Rhombohedral
M_s//<111>
MPB
Tetragonal
M_s//<001>
Temperature
Composition
(c)
Cubic
c/a>1
MPB
c/a<1
Temperature
Composition
$TbFe_2$-0.7$DyFe_2$
MPB
Above MPB
Below MPB
Magnetostriction
Magnetic field
Type-I MPB
$TbCo_2$-$GdCo_2$
off-MPB
MPB
@ 299.3 K
off-MPB
Magnetostriction
Magnetic field
Type-II MPB
$DyCo_2$-0.08$DyFe_2$
Above MPB
MPB
Below MPB
Magnetostriction
Magnetic field
Type-III MPB